(10) S. A. Johnson, H. R. Hunt, and H. M. Neuman, *Inorg. Chem.*, **2**, 960 (1963).
(11) L. Dubicki and R. L. Martin, *Inorg. Chem.*, **9**, 673 (1970).
(12) G. A. Rempel, P. Legzdins, H. Smith, and G. Wilkinson, *Inorg. Synth.*, **13**, 90 (1972).
(13) D. S. Martin, Jr., *Inorg. Chim. Acta, Rev.*, **5**, 107 (1971).
(14) This matrix, although in somewhat different form, is equivalent to the one presented by T. S. Piper, *J. Chem. Phys.*, **35**, 1240 (1961).
(15) A. P. Ketteringham and C. Oldham, *J. Chem. Soc., Dalton Trans.*, 1067 (1973).

Contribution from the Departments of Chemistry, The Pennsylvania State University, University Park, Pennsylvania 16802, and Northern Illinois University, DeKalb, Illinois 60115

Metal-to-Ligand Charge-Transfer Spectra of Some Chloro-Bridged Complexes of Rhodium(I) and Iridium(I)

RONALD A. EPSTEIN,[1a] GREGORY L. GEOFFROY,*[1a] MARK E. KEENEY,[1a] and W. ROY MASON*[1b]

Received July 7, 1978

Electronic absorption and magnetic circular dichroism (MCD) spectra are reported for the chloro-bridged dimers $[RhCl(CO)_2]_2$, $[RhCl(COD)]_2$, $[RhCl(NBD)]_2$, and $[IrCl(COD)]_2$ (COD = 1,5-cyclooctadiene; NBD = norbornadiene) in dichloromethane solution. Absorption spectra are also reported for the less stable $[RhCl(C_2H_4)_2]_2$, $[RhCl(COT)_2]_2$, and $[IrCl(COT)_2]_2$ (COT = cyclooctene) complexes. Spectra at 77 K were also obtained for $[RhCl(CO)_2]_2$ and several of the olefin complexes in glassy EPA or methylcyclohexane/pentane solution. Dissolution of $[RhCl(CO)_2]_2$, $[RhCl(COD)]_2$, $[RhCl(NBD)]_2$, and $[IrCl(COD)]_2$ in acetonitrile gives a bridge-cleavage reaction, and spectral data are reported for the monomeric products $[RhCl(CO)_2(CH_3CN)]$, $[RhCl(COD)(CH_3CN)]$, $[RhCl(NBD)(CH_3CN)]$, and $[IrCl(COD)(CH_3CN)]$. The intense bands observed in the visible and near-ultraviolet regions of the spectra of all these complexes are assigned as metal-to-ligand charge-transfer (MLCT) transitions from occupied metal d orbitals to low-energy ligand π^* orbitals. Detailed spectral assignments are presented, and comparisons are made between the chloro-bridged complexes and related monomeric complexes.

Introduction

We have recently examined the electronic absorption and magnetic circular dichroism (MCD) spectra of a series of planar d^8 complexes possessing π-acceptor ligands.[2-6] These studies have included complexes of Rh(I), Ir(I), Pd(II), and Pt(II) with ligands such as CN^-, CNR, CO, PR_3, AsR_3, and bidentate diphosphines. The low-lying bands of these complexes in the visible–near-UV spectral region have been attributed to metal-to-ligand charge-transfer (MLCT) transitions.[2-6] To further our understanding of MLCT transitions in low-valent organometallic complexes we have turned our attention to a series of chloro-bridged dimeric complexes of Rh(I) and Ir(I), many of which possess olefinic ligands. These complexes afford us the opportunity to probe the effect of the dimerization on the MLCT transitions and, further, to examine the nature of metal-to-olefin charge transfer.

The complex which we have focused most of our attention on and discuss in detail herein is $[RhCl(CO)_2]_2$. X-ray structural analysis[7] of this complex has shown it to have the bent structure shown in **1** with the two $RhCl_2(CO)_2$ planes intersecting at an angle of 124°. The *intra*molecular Rh–Rh distance is 3.12 Å, and an *inter*molecular Rh–Rh contact distance of 3.31 Å was evident between dimeric units. Infrared spectral studies[8] and dipole moment measurements[9] showed that the complex maintains its bent geometry in solution, and hence the bending must not be due to crystal packing forces but must have an electronic origin. The nature of these effects was explored in a recent SCF–Xα–SW analysis by Norman and Gmur,[10] who concluded that there is no Rh–Rh interaction through the highest occupied set of mainly 4d orbitals and that the nonlinear geometry is due to interaction of orbitals that are mainly chlorine 3p in character.

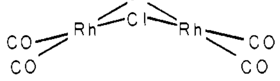

1

Of the several chloro-bridged olefin complexes which have been characterized, only two have had their structures determined by X-ray diffraction. The ethylene complex $[RhCl(C_2H_4)_2]_2$ has the bent geometry shown in **2**,[11] whereas $[RhCl(COD)]_2$ (COD = 1,5 cyclooctadiene) is planar with the olefinic bonds perpendicular to the Rh_2Cl_2 plane, **3**.[12]

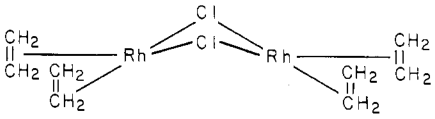

2

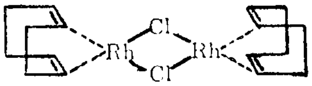

3

Definitive structural data for $[RhCl(NBD)]_2$ (NBD = norbornadiene), $[RhCl(COT)_2]_2$ (COT = cyclooctene), $[IrCl(COD)]_2$, and $[IrCl(COT)_2]_2$ are lacking. To our knowledge no information concerning solution geometries of any of these olefin complexes has been reported.

Experimental Section

The complexes $[RhCl(COD)]_2$,[13] $[RhCl(NBD)]_2$,[14] $[RhCl(COT)_2]_2$,[15] $[RhCl(C_2H_4)_2]_2$,[16] $[RhCl(CO)_2]_2$,[16] $[(n\text{-}C_4H_9)_4N][RhCl_2(CO)_2]$,[17] $[IrCl(COD)]_2$,[18] and $[IrCl(COT)_2]_2$[18] were prepared by published procedures. Electronic absorption spectra were recorded on a Cary Model 17 or a Cary Model 1501 spectrophotometer using 1.0-cm path length quartz cells. The MCD spectra were recorded on a Jasco ORD/uv-5 (equipped with CD attachment) using a permanent magnet (field 10^4 G). Spectra at 77 K were measured in frozen 5:5:2 diethyl ether/isopentane/ethanol (EPA) or 7:4 methylcyclohexane/pentane solutions using a quartz Dewar. The 77 K spectra were corrected for 26 and 20% solvent contraction, respectively.

Solutions of $[RhCl(C_2H_4)_2]_2$, $[RhCl(COT)_2]_2$, $[IrCl(COD)]_2$, and $[IrCl(COT)_2]_2$ were found to be quite air sensitive and were therefore prepared on a vacuum line or in an inert-atmosphere drybox using specially constructed degassable quartz UV cells or quartz tubes. Solvents for these solutions were dried using standard methods and degassed before use.

$[RhCl(COT)_2]_2$ rapidly decomposes even in degassed CH_2Cl_2 solution. We found that the decomposition could be slowed long enough to allow spectral measurements by adding excess COT to the solutions. However, reliable extinction coefficients and the low-temperature spectrum could not be obtained.[19] $[IrCl(COT)_2]_2$ proved to be more stable than $[RhCl(COT)_2]_2$, and degassed CH_2Cl_2 solutions

0020-1669/79/1318-0478$01.00/0 © 1979 American Chemical Society

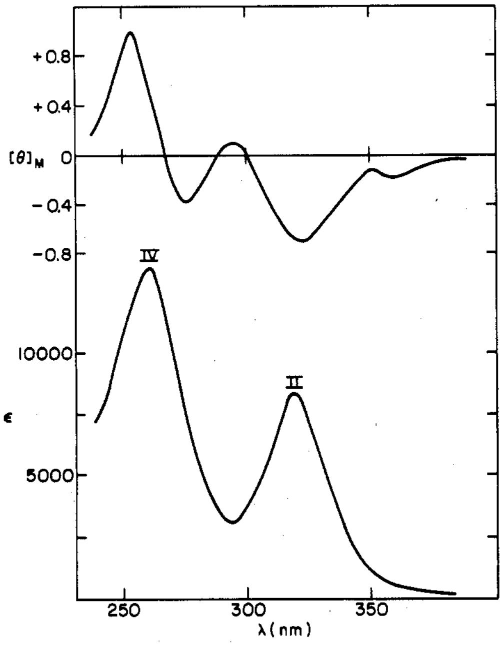

Figure 1. Electronic absorption (lower curve) and magnetic circular dichroism (upper curve) spectra of $[RhCl(CO)_2]_2$ in CH_2Cl_2 solution.

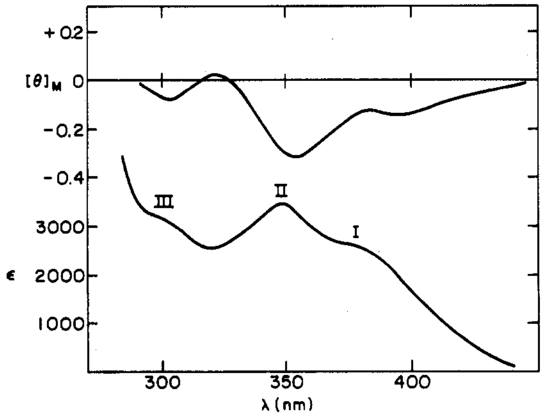

Figure 2. Electronic absorption (lower curve) and magnetic circular dichroism (upper curve) spectra of $[RhCl(COD)]_2$ in CH_2Cl_2 solution.

showed little change in the electronic absorption spectrum after 20–30 min.

Results

Electronic Absorption and MCD Spectra. Solution electronic absorption and MCD spectral data for the complexes examined are collected in Table I. Figures 1–3 are typical of the spectra obtained, and they show well-defined MCD terms for most of the observed absorption bands. In several cases the MCD spectra were better resolved than the corresponding absorption spectra. Figure 1, for example, shows a low-energy *B* term clearly resolved at 360 nm in the MCD spectrum of $[RhCl(CO)_2]_2$ in CH_2Cl_2 solution, while the corresponding band in the absorption spectrum is obscured by the intense band at 318 nm. This low-energy band was observed, however, in the absorption spectra measured in THF (370 nm) and diethyl ether (365 nm) solutions.

Electronic absorption spectra of several complexes were also measured at 77 K in glassy EPA or methylcyclohexane/pentane solutions. As illustrated in Figures 4 and 5, the bands generally sharpened and increased in intensity upon cooling to 77 K, indicative of allowed charge-transfer transitions. As can be seen in these figures, some structure was also resolved at 77 K in the spectra of $[IrCl(COD)]_2$ and $[RhCl(COD)]_2$. Measurement of the spectrum of $[RhCl(CO)_2]_2$ at 77 K in methylcyclohexane/pentane solution gave a surprising result, Figure 6. Instead of the sharpening and intensity increase observed in EPA, the spectrum showed a marked red shift

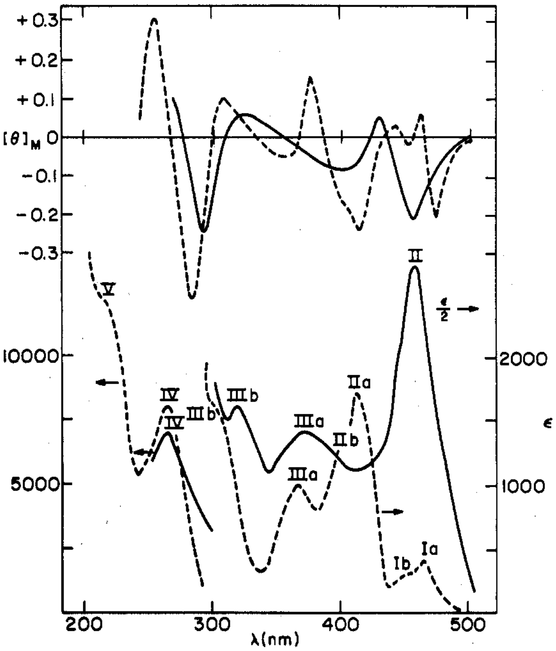

Figure 3. Electronic absorption (lower curves) and magnetic circular dichroism (upper curves) spectra of $[IrCl(COD)]_2$ in CH_2Cl_2 solution (—) and in CH_3CN solution (---) ($[IrCl(COD)(CH_3CN)]$).

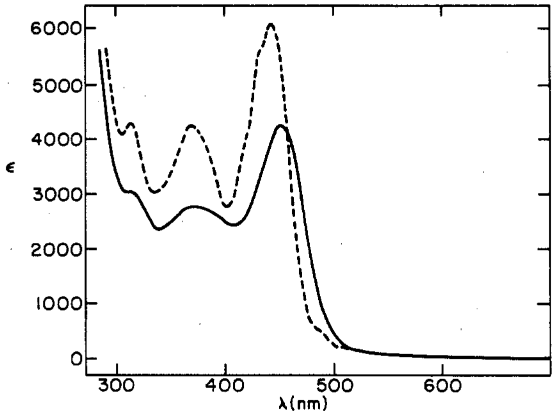

Figure 4. Electronic absorption spectra of $[IrCl(COD)]_2$ in methylcyclohexane/pentane solution at 300 K (—) and 77 K (---). The 77 K spectrum is not corrected for solvent contraction.

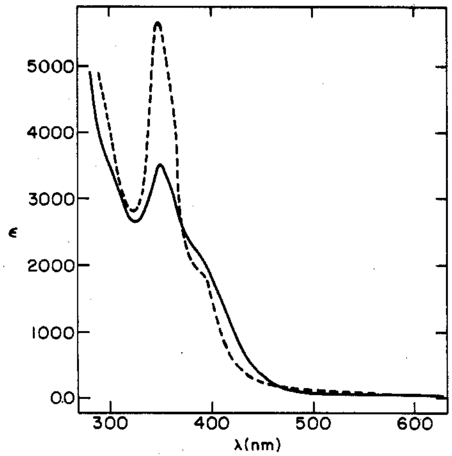

Figure 5. Electronic absorption spectra of $[RhCl(COD)]_2$ in methylcyclohexane/pentane solution at 300 K (—) and 77 K (---). The 77 K spectrum is not corrected for solvent contraction.

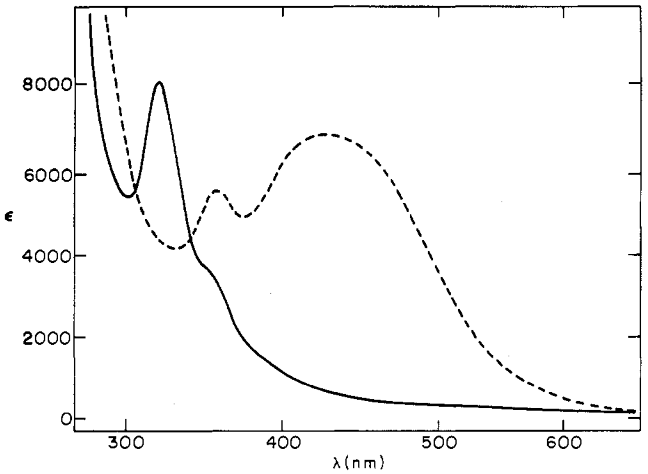

Figure 6. Electronic absorption spectra of $[RhCl(CO)_2]_2$ in methylcyclohexane/pentane solution at 300 K (—) and 77 K (---). The 77 K spectrum is not corrected for solvent contraction.

upon cooling. This and all of the 77 K spectral changes were completely reversible upon warming to 300 K.

Cleavage of the Chloro Bridges by Acetonitrile. As illustrated by the data presented in Table II, the intense 318-nm band in the absorption spectrum of $[RhCl(CO)_2]_2$ shows small but definite solvent shifts as the solvent is varied through a wide range. However, when CH_3CN is used as the solvent or is added to a CH_2Cl_2 solution of $[RhCl(CO)_2]_2$, a spectral change occurs which we interpret as indicative of a bridge-cleavage reaction to give monomeric $[RhCl(CO)_2(CH_3CN)]$. When a CH_2Cl_2 solution of $[RhCl(CO)_2]_2$ is titrated with CH_3CN, the intense band at 318 nm is replaced by a band at 334 nm. Since this change is complete as soon as there is an excess of CH_3CN over complex, a simple solvent shift can be ruled out because the mole percent of CH_3CN in the CH_2Cl_2 solution is far too small to cause a shift of the magnitude observed. The bridge-cleavage product can be recovered as a solid by evaporating the solvent. If it is immediately redissolved in pure CH_2Cl_2 the absorption spectrum is identical with that observed before evaporation. Thus, the cleavage reaction is not readily reversible. Unfortunately, the cleavage product rapidly decomposes in the solid state, and all attempts to isolate and purify a sample for complete characterization and elemental analysis have failed.[20]

A similar bridge-cleavage reaction was observed when CH_3CN was added to CH_2Cl_2 solutions of $[RhCl(COD)]_2$, $[RhCl(NBD)]_2$, and $[IrCl(COD)]_2$ or when these compounds were dissolved directly in CH_3CN. In the case of $[RhCl(COD)]_2$, titration of a CH_2Cl_2 solution with CH_3CN revealed isosbestic points for the dimer and the cleavage product at 384 and 366 nm. Further, when the solvents were evaporated and the solid was redissolved in pure CH_2Cl_2, the spectrum obtained was consistent with the dimer complex rather than the cleavage product. This contrasts with the behavior of $[RhCl(CO)_2]_2$ and suggests that the cleavage of $[RhCl(COD)]_2$ by CH_3CN is reversible. The electronic absorption and MCD spectra of $[IrCl(COD)]_2$ in CH_2Cl_2 and CH_3CN solution, Figure 3, also clearly demonstrate that two distinctly different species are present in the two solutions. This is further amplified by the spectra changes obtained upon titration of a CH_2Cl_2 solution of $[IrCl(COD)_2]$ with CH_3CN, Figure 7, which shows distinct isosbestic points at 420, 397, 310, and 297 nm.[20]

Discussion

Molecular Orbital Energy Levels and Excited States. Energy level diagrams for several planar Rh(I) and Ir(I) complexes of D_{4h} symmetry have been previously published together with the symmetry representations of the excited states expected for MLCT transitions.[2,4-6] In the discussion below we treat each metal center in the dimeric complexes as a separate chromophore having C_{2v} symmetry. The one-electron molecular orbital energy level diagram which is appropriate for this symmetry is shown in Figure 8. The coordinate system was chosen such that the x axis lies along the molecular symmetry axis, $C_2(x)$, and the z axis is perpendicular to the molecular plane. Previous studies have clearly shown that d_{z^2} ($2a_1$) is the highest occupied molecular orbital in complexes of this type and that the lowest unoccupied orbital is mainly ligand based (L_π) with some admixture of $(n + 1)p_z$.[2,4-6] In the complexes discussed herein the latter orbital is formed from either CO-π^* or olefin-π^* components and its symmetry is $2b_1$. The excited configurations and corresponding symmetry representations which arise from population of the $2b_1$ orbital are shown in Table III. The double group representations, appropriate for describing the spin–orbit states, are also given.

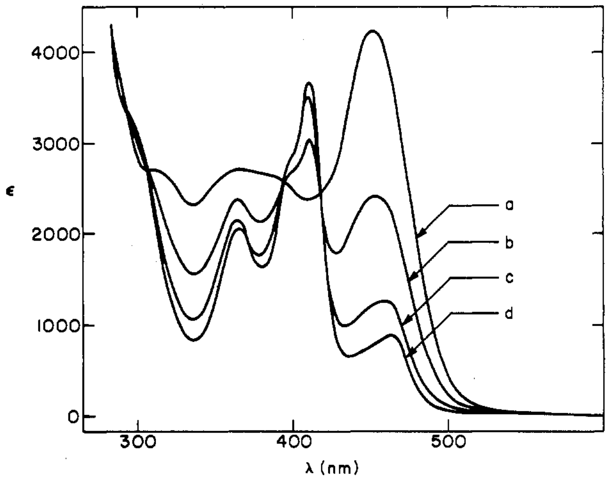

Figure 7. Spectral changes observed during titration of a CH_2Cl_2 solution of $[IrCl(COD)]_2$ with CH_3CN. Approximate % CH_3CN is (a) 0.05%, (b) 0.15%, (c) 0.25%, and (d) 1.00%.

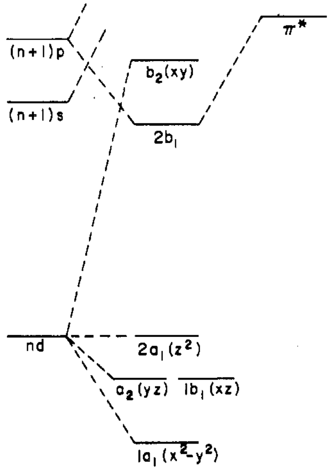

Figure 8. Molecular orbital energy level diagram appropriate for the complexes of C_{2v} symmetry discussed in the text.

The coordinates in C_{2v} symmetry transform as $a_1(x)$, $b_1(z)$, and $b_2(y)$. Therefore only transitions to $^1A_1$, $^1B_1$, and $^1B_2$ states are fully allowed by dipole selection rules. However, in the presence of spin–orbit coupling the spin-multiplicity selection rules break down, and transitions to formally triplet excited states may gain appreciable intensities by admixtures of singlet states.

MLCT Spectra. The electronic absorption spectra of $[RhCl(CO)_2]_2$ and the dimeric Rh(I) and Ir(I) olefin com-

Table I. Electronic Absorption and Magnetic Circular Dichroism Spectral Data

complex	absorption: band no.[b]	λ_{max}, nm	$\bar{\nu}_{max}$, μm^{-1}	ϵ_{max}, M^{-1} cm^{-1}	MCD: $\bar{\nu}$, μm^{-1} ($[\Theta]_M$)[a]	assignt[b]
$[(n\text{-}C_4H_9)_4N][RhCl_2(CO)_2]$[c]	II	336	2.98	2700	2.96 (−0.20)	$(d\sigma\text{-MLCT})^1$
	IV	270	3.70	5400	3.86 (+0.38)	$(d\pi\text{-MLCT})^1$
$[RhCl(CO)_2]_2$[d]	I	365[e]	2.74		2.78 (−0.18)	$(d\sigma\text{-MLCT})^3$
	II	318	3.14	8300	3.13 (−0.72)	$(d\sigma\text{-MLCT})^1$
					3.41 (+0.12)	
	IV	260	3.85	13400	3.65 (−0.38)	$(d\pi\text{-MLCT})^1$
					3.95 (+0.99)	
$[RhCl(CO)_2(CH_3CN)]$[f]	II	334	2.99	3130	2.96 (−0.37)	$(d\sigma\text{-MLCT})^1$
					3.55 (−0.14)	
	IV	257	3.89	5890	3.97 (+0.45)	$(d\pi\text{-MLCT})^1$
$[RhCl(COD)]_2$[d]	I	380	2.63	2570[g]	2.54 (−0.14)	$(d\sigma\text{-MLCT})^3$
	II	348	2.87	3500	2.84 (−0.31)	$(d\sigma\text{-MLCT})^1$
	III	300	3.33	3180[g]	3.31 (−0.08)	$(d\pi\text{-MLCT})^3$
$[RhCl(COD)(CH_3CN)]$[f]	II	373	2.68	1360		$(d\sigma\text{-MLCT})^1$
	IV	268	3.73	3260		$(d\pi\text{-MLCT})^1$
$[RhCl(NBD)]_2$[d]	I	420	2.38	1750[g]	2.43 (−0.14)[g]	$(d\sigma\text{-MLCT})^3$
	II	382	2.62	3070	2.61 (−0.29)	$(d\sigma\text{-MLCT})^1$
	IV	275	3.64	6050[g]	3.64 (+0.09)	$(d\pi\text{-MLCT})^3$
$[RhCl(NBD)(CH_3CN)]$[f]	II	397	2.52	1520		$(d\sigma\text{-MLCT})^1$
	III	300	3.33	2390		$(d\pi\text{-MLCT})^3$
	IV	278	3.61	3180		$(d\pi\text{-MLCT})^1$
$[RhCl(C_2H_4)_2]_2$[d]	I	429	2.33			$(d\sigma\text{-MLCT})^3$
	IIa	394	2.54			$(d\sigma\text{-MLCT})^1$
	IIb	380	2.63			$(d\sigma\text{-MLCT})^1$
	IV	273	3.66			$(d\pi\text{-MLCT})^1$
$[RhCl(COT)_2]_2$[d]	I	425	2.35			$(d\sigma\text{-MLCT})^3$
	II	352	2.84			$(d\sigma\text{-MLCT})^1$
$[IrCl(COD)]_2$[d]	II	455	2.20	4690	2.20 (−0.21)	$(d\sigma\text{-MLCT})^1$
					2.34 (+0.05)	
	IIIa	370	2.70	2810	2.50 (−0.09)	$(d\pi\text{-MLCT})^3$
	IIIb	319	3.13	2750	2.10 (+0.06)	$(d\pi\text{-MLCT})^3$
					3.44 (−0.24)	
	IV	265	3.77	7000		$(d\pi\text{-MLCT})^1$
$[IrCl(COD)(CH_3CN)]$[f]	Ia	463	2.16	416	[h] 2.12 (−0.20) 2.16 (0.00) 2.18 (+0.05)	$(d\sigma\text{-MLCT})^3$
	Ib	448	2.23	306[g]	[h] 2.22 (−0.02) 2.24 (0.00) 2.27 (+0.03)	$(d\sigma\text{-MLCT})^3$
	IIa	412	2.43	1720	2.43 (−0.24)	$(d\sigma\text{-MLCT})^1$
	IIb	400	2.50	1300[g]	2.48 (−0.18)[g]	$(d\sigma\text{-MLCT})^1$
	IIIa	368	2.72	1010	[h] 2.67 (+0.16) 2.74 (0.00) 2.82 (−0.05)	$(d\pi\text{-MLCT})^3$
					3.27 (+0.10)	
	IIIb	297	3.37	1610	3.37 (0.00)	$(d\pi\text{-MLCT})^3$
	IV	263	3.80	8300	[h] 3.53 (−0.42) 3.75 (0.00) 3.97 (+0.30)	$(d\pi\text{-MLCT})^1$
	V	213	4.69	12000[g]		(see text)
$[IrCl(COT)_2]_2$[d]	I	461	2.17	690		$(d\sigma\text{-MLCT})^3$
	II	417	2.40	1540		$(d\sigma\text{-MLCT})^1$
	III	370	2.70	1680		$(d\pi\text{-MLCT})^3$

[a] $[\Theta]_M = 3300(\Delta A/MlH)$, where ΔA is measured differential absorbance, M is the molar concentration, l is the path length in cm, and H is the magnetic field in gauss. [b] See text for description of this notation. [c] Data from ref 6. [d] CH_2Cl_2 solution. [e] Et_2O solution. [f] CH_3CN solution. [g] Shoulder; ϵ or $[\Theta]_M$ at the given $\bar{\nu}$. [h] Pseudo A term.

plexes closely parallel the MLCT patterns established for the monomeric complexes previously examined.[2,4–6] The signs and magnitudes of the MCD terms, the relatively intense bands which show the characteristic temperature independence, and the relative band energies leave little doubt that analogous MLCT assignments are appropriate. The spectral energy ordering Ir(I) < Rh(I) observed for the $[MCl(COD)]_2$ and $[MCl(COT)_2]_2$ dimers (Table I) is fully consistent with an MLCT assignment.[21]

To provide a basis for discussion of the spectra of the dimeric complexes, it is appropriate to briefly review the higher symmetry D_{4h} complexes previously examined.[6] Spectral data for the representative complexes $[M(Ph_2PCHCHPPh_2)_2]Cl$ (M = Rh, Ir) are set out in Table IV.[6] Two allowed MLCT band systems are observed in each case, arising from the $nd_{z^2} \rightarrow L_\pi$ and $nd_{yz}, nd_{xz} \rightarrow L_\pi$ one-electron excitations. For the Rh complexes where spin–orbit coupling is weak, the two lowest energy bands are the triplet and singlet components of the $d_{z^2} \rightarrow L_\pi$ excitation and these are followed by the triplet and singlet components of $d_{yz}, d_{xz} \rightarrow L_\pi$. A similar situation was found for the Ir complexes except that the triplet components gained considerable intensity through spin–orbit coupling. For simplicity, the transitions which derive from the $2a_1(z^2) \rightarrow 2b_1$ one-electron excitations are denoted by dσ-MLCT and those arising from $a_2(yz), 1b_1(xz) \rightarrow 2b_1$ by dπ-MLCT. Superscripts on these notations indicate singlet or triplet parentage. The transitions are numbered as follows: band I represents $(d\sigma\text{-MLCT})^3$ arising from $^1A_1 \rightarrow {}^3B_1$ (aA_1,

Table II. Effect of Solvent on the Electronic Absorption Spectrum of $[RhCl(CO)_2]_2$

solvent	$\bar{\nu}$, μm^{-1}	solvent	$\bar{\nu}$, μm^{-1}
CH_2Cl_2	3.14	$(C_2H_5)_2O$	3.06
CCl_4	3.13	THF	3.05
C_6H_5Cl	3.11	EPA, 300 K	3.05
$C_6H_5CH_3$	3.11	EPA, 77 K	3.03

solvent		
% CH_2Cl_2[a]	% THF[a]	$\bar{\nu}$, μm^{-1}
100	0	3.14
99.96	0.04	3.14
99.6	0.4	3.13
89	11	3.09
0	100	3.05

[a] % volume.

Table III. Excited Configurations and Symmetry Representations for MLCT Transitions

excited configuration[a]	excited states (no spin-orbit coupling)	double group[b] (spin-orbit coupling)
$[2a_1(z)][2b_1]$	$^1B_1$	aB_1
	$^3B_1$	aA_1, (aA_2), aB_2
$[1a_2(yz)][2b_1]$	$^1B_2$	bB_2
	$^3B_2$	bA_1, (bA_2), bB_1
$[1b_1(xz)][2b_1]$	$^1A_1$	cA_1
	$^3A_1$	(cA_2), cB_1, cB_2
$[1a_1(x^2-y^2)][2b_1]$	$^1B_1$	dB_1
	$^3B_1$	dA_1, (dA_2), dB_2

[a] Filled levels omitted. [b] Forbidden states are given in parentheses.

Table IV. Spectral Data for $[M(Ph_2PCHCHPPh_2)_2]Cl$ Complexes[a]

M	band no.	λ_{max}, nm	$\bar{\nu}_{max}$, μm^{-1}	ϵ_{max}, M^{-1} cm^{-1}	assignt
Rh	I	467	2.14	205	$^1A_{1g} \rightarrow aE_u$ $(d\sigma\text{-MLCT})^3$
	II	402	2.49	5230	$^1A_{1g} \rightarrow aA_{2u}$ $(d\sigma\text{-MLCT})^1$
	III	333 sh	3.00 sh	5860	$^1A_{1g} \rightarrow bE_u$ $(d\pi\text{-MLCT})^3$
	IV	311	3.22	8900	$^1A_{1g} \rightarrow cE_u,bA_{2u}$ $(d\pi\text{-MLCT})^1$
Ir	I	521	1.92	970	$^1A_{1g} \rightarrow aE_u$ $(d\sigma\text{-MLCT})^3$
	II	437	2.29	5100	$^1A_{1g} \rightarrow aA_{2u}$ $(d\sigma\text{-MLCT})^1$
	III	376	2.66	6000	$^1A_{1g} \rightarrow bE_u$ $(d\pi\text{-MLCT})^3$
	IV	313	3.20	9100	$^1A_{1g} \rightarrow cE_u,bA_{2u}$ $(d\pi\text{-MLCT})^1$

[a] Data from ref 6.

aB_2); band II represents $(d\sigma\text{-MLCT})^1$ from $^1A_1 \rightarrow {}^1B_1$ (aB_1); band III represents $(d\pi\text{-MLCT})^3$ arising from $^1A_1 \rightarrow {}^3B_2$, $^3A_1$ (bA_1, bB_1, cB_1, cB_2); band IV represents $(d\pi\text{-MLCT})^1$ from $^1A_1 \rightarrow {}^1B_2$, $^1A_1$ (bB_2, cA_1).

In the MCD spectra of the Rh(I) complexes where spin–orbit coupling is weak, a positive *B* term (negative ellipticity) is expected for the $(d\sigma\text{-MLCT})^3$ and $(d\sigma\text{-MLCT})^1$ transitions.[6] *B* terms are also expected for the $(d\pi\text{-MLCT})^3$ and $(d\pi\text{-MLCT})^1$ transitions for these complexes with C_{2v} symmetry. However, two overlapping *B* terms of opposite signs arising from adjacent excited states, which are close in energy and connected by a magnetic moment, will give the appearance of an *A* term. Such pseudo *A* terms are found for the dπ-MLCT transitions arising from the $a_2(yz) \rightarrow 2b_1$ and $1b_1(xz) \rightarrow 2b_1$ excitations. These transitions are strictly degenerate in the higher symmetry D_{4h} complexes, and lowering the symmetry to C_{2v} does not appear to significantly break the degeneracy. A negative *B* term will also be associated with these transitions but the pseudo *A* term appears to dominate the observed MCD in nearly every case. In the Ir(I) complexes both the absorption and MCD spectra are more complicated due to mixing of formally singlet and triplet states via spin–orbit coupling.

$[RhCl(CO)_2]_2$. Apart from a small blue shift of the dimer bands and the higher dimer absorptivities due to the presence of two Rh(I) centers per molecule (Table I), there is little difference between the spectra of the $[RhCl(CO)_2]_2$ dimer and the $[RhCl_2(CO)_2]^-$ monomeric anion, and analogous assignments are reasonable. The lower energy intense band at 318 nm in the spectrum of $[RhCl(CO)_2]_2$ is assigned to the spin-allowed dσ-MLCT transition, while the band at 260 nm is assigned to the spin-allowed dπ-MLCT transitions. As discussed previously[6] for $[RhCl_2(CO)_2]^-$, the MCD spectrum is consistent with these assignments. The weak positive *B* term resolved at 360 nm in CH_2Cl_2 solution, which corresponds to weak shoulders seen in the absorption spectra at 370 nm in THF or 365 nm in diethyl ether solutions, is assigned to a spin-forbidden component of the dσ-MLCT transition.

As recently pointed out by Balch and Tulyathan,[22] the similarity between the spectra of $[RhCl(CO)_2]_2$ and $[RhCl_2(CO)_2]^-$ indicates no significant interaction between the metal 4d orbitals on the two Rh(I) centers of the dimer. If significant interaction were present, a red shift of the out-of-plane $4d_{z^2} \rightarrow \pi^*(CO)$ transition would be expected due to the formation of bonding and antibonding combinations of the d_{z^2} orbitals and stabilization of the $\pi^*(CO)$ orbitals.[22,23] Such a red shift has in fact been found for the dσ-MLCT in Rh(I) dimer complexes in which the molecular planes are held parallel and close to one another by bridging ligands.[22-24] Our experimental data therefore indicates that the folded structure of $[RhCl(CO)_2]_2$ does not allow a close enough approach of the Rh(I) centers for there to be *significant* interaction of the metal orbitals. However, the effect of solvent on the position of the $(d\sigma\text{-MLCT})^1$ band of the dimer, Table II, suggests that there is some interaction between the two halves of the molecule. These solvent shifts are not seen in the spectra of the olefin dimers or $[RhCl_2(CO)_2]^-$ and do not correlate with the solvent dipole moments or dielectric constants. The solvent presumably affects the Rh–Rh interaction by changing the bending angle of the dimer.

In contrast to the $[RhCl(CO)_2]_2$ spectrum at room temperature or at 77 K in EPA, the 77 K spectrum in methylcyclohexane/pentane shows a marked red shift in the absorption (Figure 6). By visual inspection of this solution, it appears that the change in the spectrum occurs at the point that the solution glasses. This red shift may be due to increased metal orbital interaction caused by a forced increase in folding of the two Rh(I) planes resulting from solvent contraction on cooling to 77 K. The result is surprising, particularly in view of the normal behavior of the spectrum on cooling to 77 K in EPA. The environment about the complex is apparently quite different in the two low-temperature glassy solutions. This may not be altogether unreasonable since EPA contains ethanol and ether which are capable of hydrogen bonding and thus forming a more open structure, whereas no such specific interactions are possible in the mixture of hydrocarbons.[25]

The spectrum of the bridge-cleavage product $[RhCl(CO)_2(CH_3CN)]$ also compares favorably with that of $[RhCl_2(CO)_2]^-$ except that the higher energy band is blue shifted from 270 to 257 nm. This shift of the dπ → MLCT transition can be rationalized in terms of increased Rh(I) d_π stability on replacement of the σ, π-donor Cl^- ligand by the σ-donor CH_3CN ligand. The lower energy dσ-MLCT band involving the d_{z^2} orbital should not be sensitive to differences in ligand-π-donor ability.

Rhodium(I)–Olefin Complexes. The intense band systems with maxima at 348, 382, and 380 nm in the absorption spectra of $[RhCl(COD)]_2$, $[RhCl(NBD)]_2$, and $[RhCl(C_2H_4)_2]_2$, respectively, are analogous to the low-energy $(d\sigma\text{-MLCT})^1$ system in $[RhCl(CO)_2]_2$, and they are assigned accordingly.

The MCD spectra of the COD and NBD complexes are also similar to that of $[\mathrm{RhCl(CO)_2}]_2$, showing the characteristic positive *B* terms for the low-energy band systems. On cooling of EPA or methylcyclohexane/pentane solutions of the COD or NBD complexes to 77 K, a second band (IIa) is resolved on the long-wavelength side of these $(\mathrm{d}\sigma\text{-MLCT})^1$ transitions. This second band is apparent even at 300 K in the C_2H_4 complex: the spectrum shows well-resolved peaks at 394 and 380 nm which sharpen on cooling to 77 K in EPA. This second band in the vicinity of the band maxima is likely due to an excited-state ligand vibration. The energy difference between the two clearly resolved peaks in the $[\mathrm{RhCl(C_2H_4)_2}]_2$ spectrum is ca. 935 $\mathrm{cm^{-1}}$ which is in the range (930–1000 $\mathrm{cm^{-1}}$) of the out-of-plane deformation mode in the ground electronic state of the free ligand or in ethylene complexes.[16,26]

The $(\mathrm{d}\sigma\text{-MLCT})^1$ bands in the olefin complexes also show low-energy shoulders in the 300 K spectra at 380 nm (COD), 420 nm (NBD), and 429 nm (C_2H_4). These shoulders correspond to the spin-forbidden dσ-MLCT band in $[\mathrm{RhCl(CO)_2}]_2$ but are much more intense. It is possible that the higher intensity indicates the presence of one or more forbidden transitions which have comparable energy in the olefin complexes. These could be unresolved vibronic ligand field transitions, which would be consistent with the reductions in intensity of these bands observed on cooling.

The bands at 275 and 273 nm for the NBD and C_2H_4 complexes, respectively, have energies and intensites similar to those of the spin-allowed dπ-MLCT transition in $[\mathrm{RhCl(CO)_2}]_2$ and are assigned as such. The shoulder at 300 nm in the spectrum of the COD complex is presumably due to a spin-forbidden dπ-MLCT transition with the spin-allowed transition obscured by the intense absorption at higher energy.

The bridge-cleavage products $[\mathrm{RhCl(COD)(CH_3CN)}]$ and $[\mathrm{RhCl(NBD)(CH_3CN)}]$ each show two intense bands in their spectra, and these are assigned in analogy to $[\mathrm{RhCl(CO)_2(CH_3CN)}]$ to the $(\mathrm{d}\sigma\text{-MLCT})^1$ and $(\mathrm{d}\pi\text{-MLCT})^1$ transitions.

Iridium(I)–Olefin Complexes. Both the absorption and MCD spectra obtained for $[\mathrm{IrCl(COD)}]_2$ in CH_2Cl_2 solution are considerably different from the spectra of the rhodium(I)–olefin complexes. The spectra of the bridge-cleavage product $[\mathrm{IrCl(COD)(CH_3CN)}]$ are complex but are virtually identical with those observed for other monomeric, square-planar Ir(I) complexes containing π-acceptor ligands.[6] The spectral assignments for this complex will be discussed first and then used to assist the interpretation of the spectrum of $[\mathrm{IrCl(COD)}]_2$.

Application of our previous model which includes Ir(I) spin–orbit coupling[6] to the absorption and MCD data for $[\mathrm{IrCl(COD)(CH_3CN)}]$ leads to the following MLCT spectral assignments. Band I at 463 nm is assigned as $(\mathrm{d}\sigma\text{-MLCT})^3$, while the more intense band II at 412 nm is assigned as the $(\mathrm{d}\sigma\text{-MLCT})^1$ transition. Bands IIIa and IIIb, at 368 and 297 nm, are assigned to components of the $(\mathrm{d}\pi\text{-MLCT})^3$ transition, and the intense band IV at 263 nm is assigned to the $(\mathrm{d}\pi\text{-MLCT})^1$ transition. The short-wavelength shoulders at 448 nm (Ib) and 400 nm (IIb) are assigned as excited-state ligand vibrations associated with the triplet and singlet dσ-MLCT transitions, respectively. In both cases the shoulders are ca. 700 $\mathrm{cm^{-1}}$ higher in energy than the band maxima, and the MCD spectrum shows the same type of term for the shoulders as for the maxima. A high-energy shoulder (V) is also observed at 213 nm which is tentatively assigned as the allowed dπ-MLCT transition derived from the triplet $5d_{x^2-y^2} \rightarrow \pi^*$(COD).

The MCD spectrum of a CH_2Cl_2 solution of $[\mathrm{IrCl(COD)}]_2$ shows a prominent positive *B* term associated with the 455-nm band which resembles that observed for the spin-allowed dσ-MLCT transition in $[\mathrm{IrCl(COD)(CH_3CN)}]$, and we suggest a similar assignment. However, the band has gained intensity and is significantly red shifted from the corresponding 412-nm band of $[\mathrm{IrCl(COD)(CH_3CN)}]$. We interpret this red shift and intensity increase to be indicative of Ir–Ir interaction in the dimer solution which may be caused by folding of the dimer sufficiently to cause interaction of the out-of-plane metal orbitals. The bands IIIa and IV at 370 and 265 nm in the dimer spectra are assigned as components of the $(\mathrm{d}\pi\text{-MLCT})^3$ and $(\mathrm{d}\pi\text{-MLCT})^1$ transitions and are virtually unshifted from the corresponding bands in the monomeric cleavage product. Band IIIb at 319 nm presumably corresponds to the 297-nm band of $[\mathrm{IrCl(COD)(CH_3CN)}]$ and is assigned as one of the $(\mathrm{d}\pi\text{-MLCT})^3$ components. At 77 K in glassy methylcyclohexane/pentane solution a weak shoulder is resolved at 487 nm which is attributed to $(\mathrm{d}\sigma\text{-MLCT})^3$. Two intense shoulders are also resolved on the short-wavelength side of the 455-nm band which are probably due to excited-state ligand vibrations.

Table V. MLCT Transition Energies[a] in Rh(I) and Ir(I) Complexes

	Rh(I)			Ir(I)		
complex	σ-MLCT	π-MLCT	$\Delta_{\pi-\sigma}$	σ-MLCT	π-MLCT	$\Delta_{\pi-\sigma}$
$[\mathrm{MCl(CO)_2}]_2$	3.14	3.85	0.71			
$[\mathrm{MCl_2(CO)_2}]^-$ [b]	2.98	3.70	0.72	2.85	3.86	1.01
$[\mathrm{MCl(COD)}]_2$	2.87			2.20	3.77	1.57[d]
$[\mathrm{MCl(COD)(CH_3CN)}]$	2.68	3.73	1.05	2.43	3.80	1.37
$[\mathrm{MCl(NBD)}]_2$	2.62	3.64	1.02			
$[\mathrm{MCl(NBD)(CH_3CN)}]$	2.52	3.61	1.09			
$[\mathrm{M(CNEt)_4}]^+$ [c]	2.63	3.25	0.62	2.38	3.25	0.87
$[\mathrm{M(Ph_2PCHCHPPh_2)_2}]^+$ [b]	2.49	3.22	0.73	2.29	3.20	0.91
$[\mathrm{M(Ph_2PCH_2CH_2PPh_2)_2}]^+$ [b]	2.48	3.19	0.71	2.28	3.18	0.90

[a] In $\mu\mathrm{m}^{-1}$. [b] Reference 6. [c] Reference 4. [d] Ir–Ir interaction lowers the energy of π-MLCT and thus makes $\Delta_{\pi-\sigma}$ anomalously large (see text).

In contrast to $[\mathrm{IrCl(COD)}]_2$, the absorption spectrum of $[\mathrm{IrCl(COT)_2}]_2$ resembles the spectra of the Rh dimers and similar assignments are suggested. The bands are red shifted somewhat as expected for MLCT transitions in moving from Rh(I) to Ir(I).

Electronic Structure. Except for $[\mathrm{RhCl(CO)_2}]_2$ in methylcyclohexane/pentane at 77 K, the Rh(I) dimer complexes examined in this work show MLCT spectra analogous to those of monomeric Rh(I) complexes. Thus the electronic structure of the dimers can be described in terms of two virtually independent and identical chromophore units within the molecule. In contrast, the MLCT spectrum for $[\mathrm{IrCl(COD)}]_2$ is altered from that of normal monomeric Ir(I) complexes, and these changes are ascribed to some degree of Ir–Ir interaction.

The MLCT assignments for $[\mathrm{RhCl(CO)_2}]_2$ and the rhodium(I)– and iridium(I)–olefin complexes are made using the same ordering of MLCT excited states as for a number of other planar Rh(I) and Ir(I) complexes containing π-acceptor ligands. If differences in electronic repulsion in these MLCT states (which are presumed small) are ignored, the relative energies of the dσ- and dπ-MLCT band systems in each complex are related to the relative energies of the occupied $n\mathrm{d}_{z^2}$ and $n\mathrm{d}_{xz}$, $n\mathrm{d}_{yz}$ molecular orbitals. Data for the dσ- and dπ-MLCT transition energies together with their difference, $\Delta_{\pi-\sigma}$, for several Rh(I) and Ir(I) complexes are presented in Table V.

Cogent arguments have been advanced[3] describing the $n\mathrm{d}_{z^2}$ orbital as virtually nonbonding or only weakly antibonding. The more stable $n\mathrm{d}_{xz}$, $n\mathrm{d}_{yz}$ orbitals are bonding in nature. Thus the energy of the dσ-MLCT transition in these compounds is primarily related to the energy of the ligand-based acceptor orbital, and $\Delta_{\pi-\sigma}$ is related to the extent of metal-to-ligand π bonding. From the dσ-MLCT data shown in Table V, the ordering of the stability of the ligand acceptor orbitals is P-donor > CNR ~ olefin > CO. The energy difference between the most stable (lowest energy) P-donor ligands and the least stable CO is 0.5–0.6 μm^{-1} and is not exceptionally large. This result may imply a significant amount of metal $(n + 1)p_z$ character in the acceptor MO, since greater $(n + 1)p_z$ character would reduce the sensitivity of the orbital to the nature of the ligand. The magnitude of $\Delta_{\pi-\sigma}$ shows the order olefin > CO > PR_3 ~ CNR and suggests the olefin ligands are the best acceptor ligands of those represented in Table V. Their participation in metal-to-ligand bonding (back-bonding) causes the largest "splitting" of the occupied *n*d orbitals. Again the energy difference between the olefins and CNR is not large, amounting to only 0.40–0.42 μm^{-1}. The small "splitting" of the occupied orbitals by π-acceptor ligands has been noted previously and appears characteristic of electron-rich low coordination number complexes.[3,4,6,27]

Acknowledgment. We thank the National Science Foundation (Grant CHE 7505909) for support of this research. G.L.G. gratefully acknowledges the Camille and Henry Dreyfus Foundation for a Teacher-Scholar grant and the Alfred P. Sloan Foundation for a research fellowship.

Registry No. $[RhCl(CO)_2]_2$, 14404-25-2; $[RhCl(CO)_2(CH_3CN)]$, 68474-99-7; $[RhCl(COD)]_2$, 12092-47-6; $[RhCl(COD)(CH_3CN)]$, 68475-00-3; $[RhCl(NBD)]_2$, 12257-42-0; $[RhCl(NBD)(CH_3CN)]$, 68525-24-6; $[RhCl(C_2H_4)_2]_2$, 12081-16-2; $[RhCl(COT)_2]_2$, 12279-09-3; $[IrCl(COD)]_2$, 12112-67-3; $[IrCl(COD)(CH_3CN)]$, 68475-01-4; $[IrCl(COT)_2]_2$, 12246-51-4.

References and Notes

(1) (a) The Pennsylvania State University. (b) Northern Illinois University.

(2) G. L. Geoffroy, M. S. Wrighton, G. S. Hammond, and H. B. Gray, *J. Am. Chem. Soc.*, **96**, 3105 (1974).

(3) H. Isci and W. R. Mason, *Inorg. Chem.*, **14**, 905 (1975).

(4) H. Isci and W. R. Mason, *Inorg. Chem.*, **14**, 913 (1975).

(5) R. Brady, B. R. Flynn, G. L. Geoffroy, H. B. Gray, J. Peone, Jr., and L. Vaska, *Inorg. Chem.*, **15**, 1485 (1976).

(6) G. L. Geoffroy, H. Isci, J. Litrenti, and W. R. Mason, *Inorg. Chem.*, **16**, 1950 (1977).

(7) L. F. Dahl, C. Martell, and D. L. Wampler, *J. Am. Chem. Soc.*, **83**, 1761 (1961).

(8) J. G. Bullitt and F. A. Cotton, *Inorg. Chim. Acta*, **5**, 637 (1971).

(9) C. W. Garland and J. R. Wilt, *J. Chem. Phys.*, **36**, 1094 (1962).

(10) J. G. Norman, Jr., and D. J. Gmur, *J. Am. Chem. Soc.*, **99**, 1446 (1977).

(11) K. Klanderman and L. F. Dahl, quoted in *J. Am. Chem. Soc.*, **91**, 7292 (1969); K. Klanderman, *Diss. Abstr.*, **25**, 6353 (1965).

(12) J. A. Ibers and R. G. Snyder, *J. Am. Chem. Soc.*, **84**, 495 (1962).

(13) J. Chatt and L. M. Venanzi, *J. Chem. Soc.*, 4735 (1957).

(14) E. W. Able, M. A. Bennett, and G. Wilkinson, *J. Chem. Soc.*, 3178 (1959).

(15) A. van der Ent and A. L. Onderdelinden, *Inorg. Synth.*, **14**, 93 (1973).

(16) R. Cramer, *Inorg. Synth.*, **15**, 14 (1974).

(17) M. J. Cleare and W. P. Griffith, *J. Chem. Soc. A*, 2788 (1970).

(18) J. L. Herde, J. C. Lambert, and C. V. Senoff, *Inorg. Synth.*, **15**, 18 (1974).

(19) The electronic absorption spectrum of $[RhCl(COT)_2]_2$ was recently reported by I. Kinoshita, Y. Terai, K. Kashiwabara, H. Kido, and K. Saito, *J. Organomet. Chem.*, **127**, 237 (1977), but no mention was made of its instability. Their spectrum was markedly different from that which we obtained and could be attributed to decomposition.

(20) Related cationic complexes are known: $[Rh(CO)_2(CH_3CN)_2]^+$, R. R. Schrock and J. A. Osborne, *J. Am. Chem. Soc.*, **93**, 3089 (1971); $[Rh(COD)(CH_3CN)_2]^+$, $[Rh(NBD)(CH_3CN)_2]^+$, and $[Ir(COD)(CH_3CN)_2]^+$, M. Green, T. A. Kuc, and S. H. Taylor, *J. Chem. Soc. A*, 2334 (1971).

(21) The lowest energy intense bands in the spectra of the related $[PdCl_2(COD)]$, $[PdCl_2(NBD)]$, and $[PtCl_2(COD)]$ complexes are higher in energy than the lowest energy bands of the respective $[RhCl(COD)]_2$, $[RhCl(NBD)]_2$, and $[IrCl(COD)]_2$ dimers (R. A. Epstein and G. L. Geoffroy, unpublished observations). The energy orderings Rh < Pd and Ir < Pt are supportive of the MLCT assignments.

(22) A. L. Balch and B. Tulyathan, *Inorg. Chem.*, **16**, 2840 (1977).

(23) K. R. Mann, J. G. Gordon, II, and H. B. Gray, *J. Am. Chem. Soc.*, **97**, 3553 (1975).

(24) K. R. Mann, N. S. Lewis, V. M. Miskowski, D. K. Erwin, G. S. Hammond, and H. B. Gray, *J. Am. Chem. Soc.*, **99**, 5525 (1977).

(25) A reviewer made the reasonable suggestion that the red shift shown in Figure 6 might arise from association of separate dimer units via Rh–Rh interactions or even from formation of small crystallites upon cooling. However, the red shift was not apparent in spectra of solid samples of $[RhCl(CO)_2]_2$ dispersed in Nujol and in KBr disks in which such interactions should be enhanced.

(26) J. Chatt, L. A. Duncanson, and R. G. Guy, *Nature (London)*, **184**, 526 (1959).

(27) W. Roy Mason, *J. Am. Chem. Soc.*, **98**, 5182 (1976).

Contribution from the Department of Chemistry,
Purdue University, West Lafayette, Indiana 47907

X-ray Photoelectron Spectra of Inorganic Molecules. 22.[1] Halogen Core Electron Binding Energies of Low Oxidation State Molybdenum Bromide and Molybdenum Iodide Clusters and Niobium and Tantalum Chlorides Containing the $[M_6Cl_{12}]^{n+}$ Cores

S. A. BEST and R. A. WALTON*

Received August 31, 1978

The Br 3p and I 3d binding energy spectra of α-molybdenum bromide and iodide, $(Mo_6X_8)X_4$, and the bromide derivatives $(Mo_6Br_8)Br_4L_2$ and $(Et_4N)_2[(Mo_6Br_8)X_6]$, where X = Cl or Br, show that bridging (X_b) and terminal (X_t) halogen environments are readily differentiated by X-ray photoelectron spectroscopy (XPS). Values of $\Delta E(X_b-X_t)$ were in the range of 1.8–2.4 eV for the bromide complexes and 1.3 eV for $(Mo_6I_8)I_4$. XPS data for the complex $(Bu_4N)_2Mo_4I_{11}$ show the presence of two sets of I $3d_{3/2,5/2}$ doublets which differ in binding energy by 1.2 eV. The energies and relative intensities of these latter peaks are in accord with a stoichiometric ratio $I_b{:}I_t$ equal to 7:4. These studies constitute the first examples of the use of XPS to successfully distinguish different halogen environments in transition-metal bromides and iodides and their complexes. The Cl 2p spectra of the niobium and tantalum chloride clusters which contain the $(M_6Cl_{12})^{n+}$ cores have also been measured and show that, like Re_3Cl_9 and $(Mo_6Cl_8)Cl_4$ and their derivatives, the binding energy order is $Cl_b > Cl_t$, with $\Delta E(Cl_b-Cl_t)$ being between 1.4 and 2.1 eV.

Introduction

The steadily increasing accumulation of data on the X-ray photoelectron spectra (XPS) of metal halides and their complexes has prompted two recent reviews on this subject.[2,3] Largely as a result of work carried out in our laboratory, it has been demonstrated that for metal–metal bonded dimers and clusters which contain both bridging (Cl_b) and terminal (Cl_t) metal–chlorine bonds the Cl 2p binding energy order is $Cl_b > Cl_t$.[4-7] The chemical shift differences between $E(Cl_b)$ and $E(Cl_t)$ depend upon the system in question, ranging from ~2.3 eV for $(Mo_6Cl_8)Cl_4$ and its derivatives[6] to ~1.4 eV for Re_3Cl_9 and its derivatives[4-6] to a value between 0.5 and 1.2

0020-1669/79/1318-0484$01.00/0